



IMAGE QUALITY EVALUATION OF $\text{YVO}_4:\text{Eu}$ PHOSPHOR SCREENS FOR USE IN X-RAY MEDICAL IMAGING DETECTORS

I. KANDARAKIS,¹ D. CAVOURAS,^{1*} E. KANELLOPOULOS,¹ C. D. NOMICOS² and G. S. PANAYIOTAKIS¹

¹Department of Medical Instrumentation Technology, ²Department of Electronics, Technological Educational Institution of Athens, Agiou Spyridonos Street, Aigaleo 122 10, Athens, Greece and

³Department of Medical Physics, Medical School, University of Patras, 265 00 Patras, Greece

(Received 8 December 1997; revised 3 March 1998; accepted 8 March 1998)

Abstract— $\text{YVO}_4:\text{Eu}$ is a phosphor material emitting red light (621 nm) and providing excellent spectral compatibility with red sensitive optical detectors. However, it has never been used in medical X-ray imaging. In this study the imaging performance of six laboratory prepared $\text{YVO}_4:\text{Eu}$ test screens with coating weights from 30 to 140 mg/cm² was examined by evaluating the modulation transfer function (MTF), the X-ray luminescence efficiency (XLE), and the detective quantum efficiency (DQE). DQE was evaluated by employing a method based on XLE and emission spectra measurements. The 30 mg/cm² screen had a significantly higher MTF than thicker screens while its zero frequency DQE peak value was 0.27 at 30 kVp. Results obtained indicate that $\text{YVO}_4:\text{Eu}$ may be of value for use in X-ray imaging detectors. © 1998 Elsevier Science Ltd. All rights reserved

1. INTRODUCTION

Europium activated yttrium vanadate ($\text{YVO}_4:\text{Eu}^{3+}$) is a phosphor material which, when irradiated, emits red light at 621 nm due to the presence of Eu^{3+} ion activator. In a previous study (Panayiotakis *et al.*, 1996) data on light output and spectral compatibility of $\text{YVO}_4:\text{Eu}^{3+}$ with various light photon detectors have been reported. In that study, $\text{YVO}_4:\text{Eu}^{3+}$ emission spectrum was found to have excellent spectral matching with films sensitive to red light. Also, the sensitivity of the silicon photodiode employed in digital imaging detectors (Gurvich, 1995; Yaffe and Rowlands, 1997) matched the $\text{YVO}_4:\text{Eu}^{3+}$ spectrum better than the spectra of commonly used phosphors (Kandarakis *et al.*, 1997a; Panayiotakis *et al.*, 1996). To our knowledge, $\text{YVO}_4:\text{Eu}^{3+}$ has never been used in X-ray imaging screens or in other types of radiation detectors for medical imaging. In the present study, the imaging performance of the laboratory prepared $\text{YVO}_4:\text{Eu}^{3+}$ screens was experimentally examined to evaluate the suitability of this material to be used in conventional or digital X-ray imaging. The following parameters were evaluated:

1. The modulation transfer function (MTF) that describes the diagnostic signal modulation, or high contrast, as a function of spatial frequency

and determines the resolution limit of an imaging system.

2. The X-ray luminescence efficiency (XLE) that gives the light energy flux emitted by the phosphor per unit of incident X-ray energy flux affecting image brightness and quantum noise.
3. The detective quantum efficiency (DQE) that expresses the image information content (Shaw, 1963; Shaw and Van Metter, 1984) as described by the signal-to-noise ratio (SNR) transfer from the input to the output of an imaging system:

$$\text{DQE} = [\text{SNR}_{\text{out}}/\text{SNR}_{\text{in}}]^2. \quad (1)$$

DQE evaluation was based (Kandarakis *et al.*, 1997b) on the determination of MTF, XLE, quantum detection efficiency (QDE) and the energies of the incident X-ray photons and emitted light photons.

2. MATERIALS AND METHODS

The phosphor screens used in our experiments had coating weights of approx. 30, 60, 80, 100, 120 and 140 mg/cm², thus covering the range often used in X-ray imaging. All screens were prepared in our

*Author to whom correspondence should be addressed: Prof. D Cavouras, 37–39 Esperidon Street, Kallithea 17671, Athens, Greece. Fax: (+ 301) 5910 975; e-mail: cavouras@hol.gr, cavouras@medisp.teiath.gr

laboratory by sedimentation of $\text{YVO}_4:\text{Eu}^{3+}$ phosphor powder on silica substrates, following a preparation procedure described in previous studies (Kandarakis *et al.*, 1996; Cavouras *et al.*, 1996; Panayiotakis *et al.*, 1996). The mean size of the powder grains was $7\ \mu\text{m}$. Screens produced in this way were of granular structure with phosphor packing density slightly exceeding 50%. This screen type is very similar to that commonly used in medical radiography (Arnold, 1979; Zweig and Zweig, 1983). A drawback of granular screens is that their imaging characteristics are highly affected by light spread. The latter is due to the isotropic light propagation within the phosphor material and to the light scattering effects on powder grains. Light spread broadens the spatial distribution of emitted photons on the screen's emitting surface. Thus, the width of the point spread function (PSF), expressing spatial resolution, increases resulting in lower MTF values (Yaffe and Rowlands, 1997).

MTF was measured using 30 kVp molybdenum spectrum and 80 kVp tungsten spectrum X-rays. The technique applied for MTF determination was based on the square wave response function (SWRF) method (Barnes, 1979; Cavouras *et al.*, 1996; Kandarakis *et al.*, 1997b). Screens were used with the Agfa Scopix LT2B film, which is very sensitive to red light emitted by $\text{YVO}_4:\text{Eu}^{3+}$. The spectral matching factor of this screen-film combination has been previously determined to be 0.956 (Panayiotakis *et al.*, 1996). This is the greatest value found in our laboratory as compared to other phosphor-film combinations (Giakoumakis, 1991). To measure the SWRF, a suitable test pattern, type-53 of Nuclear Associates, was imaged by each screen film combination. The test pattern comprised Pb line pairs with spatial frequencies ranging from 2.5 to 100 line-pairs per cm. Two modes of measurements were followed: (1) Front screen configuration (transmission mode) and (2) back screen configuration (reflection mode). In the first mode, the test pattern was put in contact with the front side of the screen while the back side of the screen was in contact with the photosensitive surface of the film. In such configuration, X-rays after being transmitted through the pattern interact with the phosphor material to produce light for exposing the film. This configuration is employed in digital radiography detectors, in fluoroscopy, and in front screens of radiographic cassettes. In the second mode, a test pattern-film-phosphor material configuration was used. This setup simulates mammographic conditions and rear screens of conventional radiographic cassettes. Film images were digitized by a Microtec Scanmaker II SP (24 bit color, 1200×1200 dpi) CCD scanner. SWRFs were obtained by summing up 64 successive image traces transverse to the pattern lines from each digitized image in order to reduce noise (Cavouras *et al.*, 1996). The corresponding MTFs were then

calculated employing Coltman's formula (Barnes, 1979):

$$\text{MTF}(\omega) = \frac{\pi}{4} \left[\frac{\text{SWRF}(\omega)}{\omega} + \frac{\text{SWRF}(3\omega)}{3\omega} - \frac{\text{SWRF}(5\omega)}{5\omega} + \dots \right] \quad (2)$$

This MTF was divided by the scanner's MTF measured by scanning the pattern alone (Cavouras *et al.*, 1996). The result obtained was the screen MTF, since the film's MTF was considered equal to unity for spatial frequencies up to 100 lines per cm (Beutel *et al.*, 1993).

The X-ray luminescence efficiency was determined as the quotient of the emitted light energy flux over the incident X-ray energy flux [see formula (A3) in the appendix]. The emitted light energy flux was measured by an EMI 9558QB photomultiplier after irradiating each screen by 30 and 80 kVp X-rays. The output current of the photomultiplier was measured by a Cary 401 vibrating reed electrometer and it was converted into light energy flux ($\mu\text{W}/\text{cm}^2$) employing manufacturer's photosensitivity data, which were also verified in our laboratory employing appropriate light sources. These data give the output current per unit of incident light energy flux. The incident X-ray energy flux was determined from exposure rate measurements. Exposure rate data were converted into X-ray energy flux using the appropriate conversion factor (Hendee, 1970; Motz and Danos, 1978).

DQE(ω) was experimentally determined at 30 and 80 kVp according to the formula (Kandarakis *et al.*, 1997b):

$$\text{DQE}(\omega) = \frac{\eta_Q \eta_\phi [\bar{E}/E_\lambda] [\text{MTF}]^2}{\eta_Q + \eta_\phi [\bar{E}/E_\lambda] [\text{MTF}]^2} \quad (3)$$

where η_Q is the X-ray quantum detection efficiency giving the fraction of incident X-rays interacting with the screen material. η_ϕ is the X-ray luminescence efficiency. E_λ is the energy of the emitted light photon and \bar{E} is the average X-ray energy of the incident X-ray beam. Derivation of formula (3) is given in the Appendix.

E_λ was determined from emission spectrum measurements performed with an Oriol 7240 grating monochromator. η_Q was calculated by the formula:

$$\eta_Q = \frac{\int_0^{E_0} S_X(E) (1 - e^{-\mu(E)w}) dE}{\int_0^{E_0} S_X(E) dE} \quad (4)$$

where $S_X(E)$ is the X-ray energy spectrum calculated as described in previous studies (Tucker *et al.*, 1991a,b; Cavouras *et al.*, 1996), E_0 is the maximum X-ray energy determined by the tube voltage, $\mu(E)$ is the X-ray attenuation coefficient for $\text{YVO}_4:\text{Eu}$

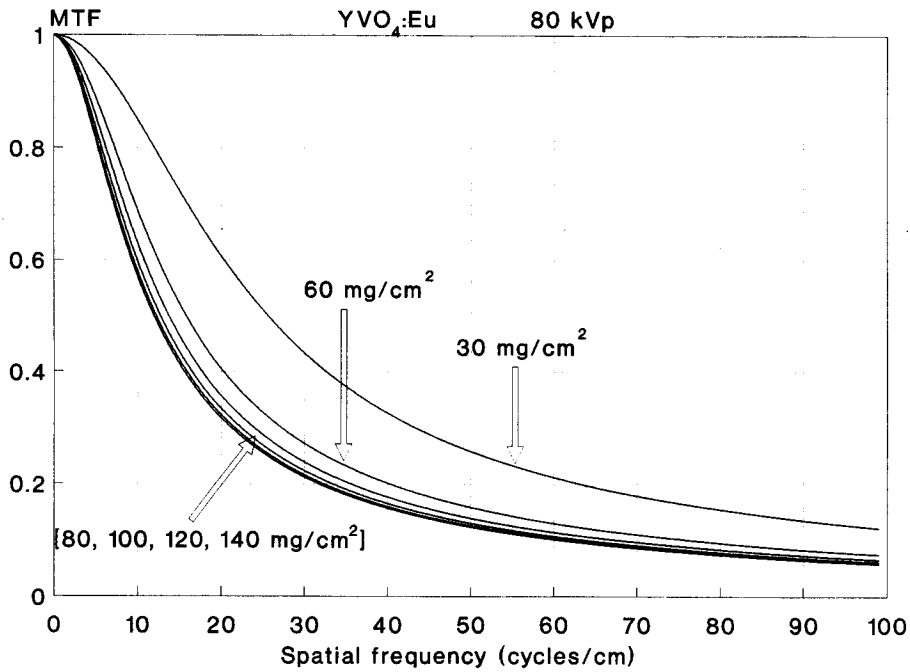


Fig. 1. MTF curves of $YVO_4:Eu$ screens measured at 80 kVp X-ray tube voltage in front screen configuration.

calculated according to data given by Storm and Israel (1967) and was the screen coating weight.

3. RESULTS AND DISCUSSION

Figure 1 shows the MTF curves of the 30, 60, 80, 100, 120 and 140 mg/cm² $YVO_4:Eu$ screens

measured at 80 kVp X-ray tube voltage in front screen configuration. The 30 mg/cm² screen shows a notably better MTF curve expressing the high resolution performance of this screen. This was expected since in thin screens light penetrates short distances to exit the phosphor material and, thus, light spread is less significant than in thicker screens.

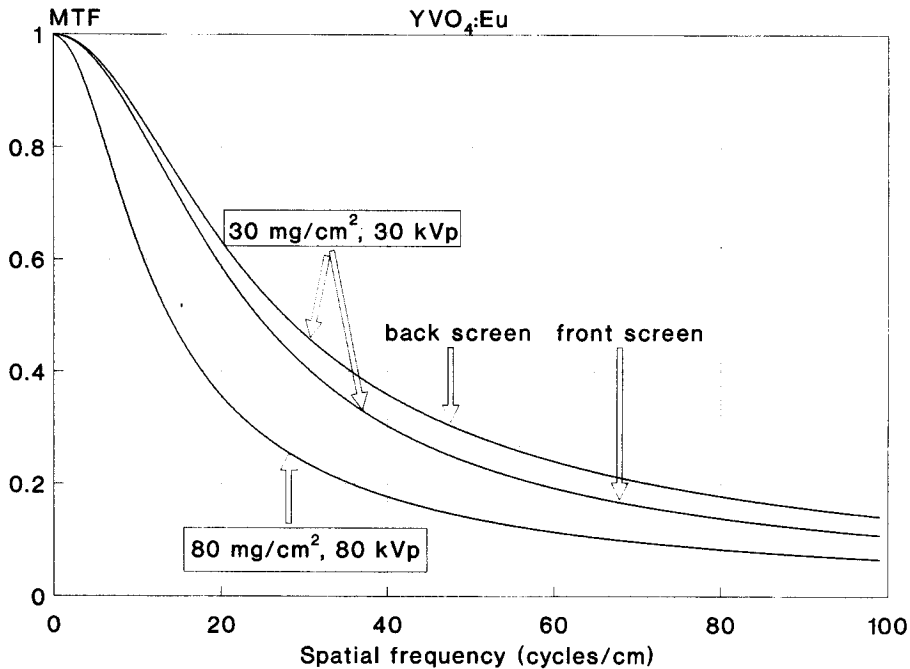


Fig. 2. MTF curves of the 30 mg/cm² $YVO_4:Eu$ screen measured at 30 kVp in front and back screen configuration mode and MTF curve of the 80 mg/cm² $YVO_4:Eu$ screen measured at 80 kVp in front screen configuration.

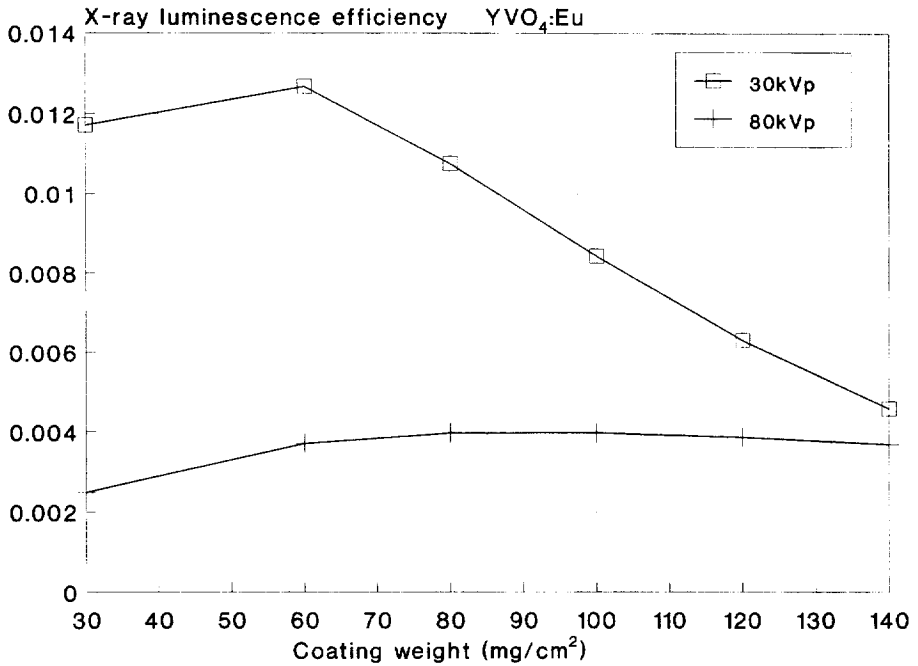


Fig. 3. X-ray luminescence efficiency of YVO₄:Eu screens measured at 30 and 80 kVp in front screen configuration.

In Fig. 2 the MTFs of the 30 and 80 mg/cm² screens measured at 30 and 80 kVp, respectively, are shown so as to compare the imaging performance obtained under mammographic (30 kVp, 30 mg/cm²) and under general radiographic conditions (80 kVp, 80 mg/cm²). The two curves shown for the 30 mg/cm² correspond to the front screen and back screen configurations. Back screen set-up

exhibits better MTF since light photons, mainly produced near the exposed phosphor surface, travel shorter distances to escape from the irradiated surface than from the non irradiated side. Hence, light spread is less significant and consequently spatial resolution is better in back screen measurements. The 30 mg/cm² front screen MTF measured at 30 kVp is slightly lower than the MTF of the same

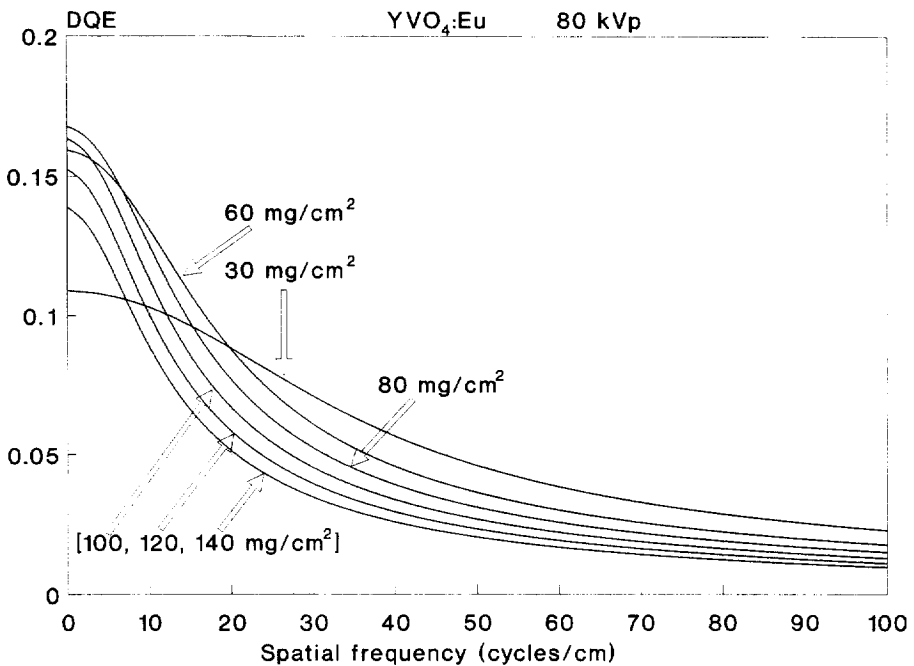


Fig. 4. DQE(ω) curves of YVO₄:Eu screens measured at 80 kVp in front screen configuration.

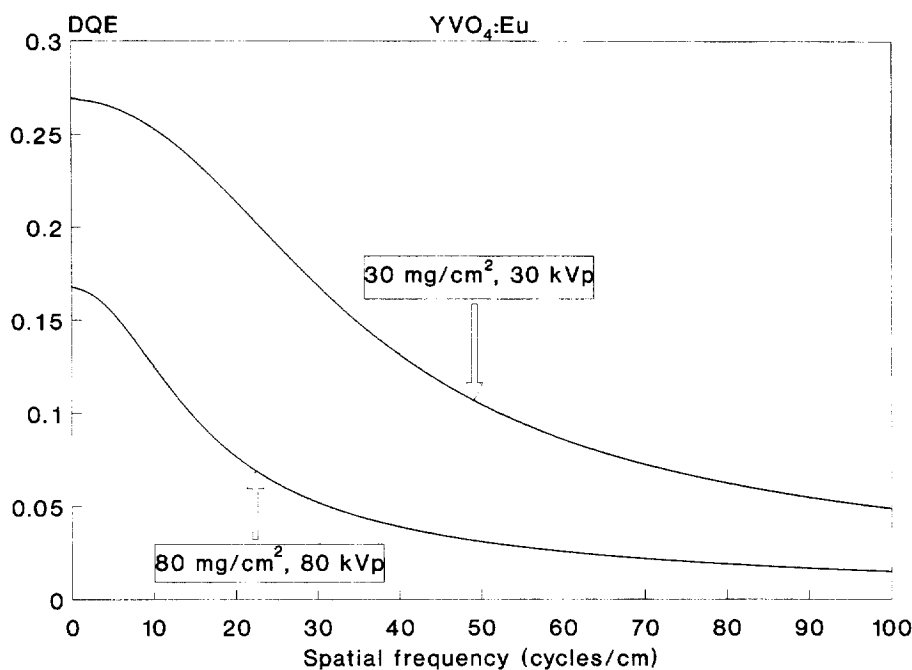


Fig. 5. Comparison of the $\text{DQE}(\omega)$ of the 30 mg/cm^2 $\text{YVO}_4:\text{Eu}$ screen measured at 30 kVp with the $\text{DQE}(\omega)$ of the 80 mg/cm^2 $\text{YVO}_4:\text{Eu}$ screen measured at 80 kVp.

screen at 80 kVp. This difference must be due to the emission of K -characteristic radiation which degrades MTF. The presence of this radiation is more significant at 30 kVp than at 80 kVp, since the K -absorption edge of yttrium is at 17 keV, which is closer to the mean energy of the 30 kVp beam.

Figure 3 shows data obtained for XLE at 30 and 80 kVp. As it is observed the $\text{YVO}_4:\text{Eu}$ XLE values are considerably higher at 30 kVp than at 80 kVp. The reason for this is that at 30 kVp the mean energy of the X-ray beam is close to the K -absorption edge of yttrium. Thus, a large fraction of the energy, conveyed by the beam, is absorbed within the phosphor and it is converted into light. As screen coating weight increases the X-ray absorption also increases producing higher numbers of emitted photons. However, emitted photon losses are significant due to longer distances that emitted photons have to travel in thicker screens before reaching the emitting surface. Thus, after a maximum value attained at 60 mg/cm^2 , XLE decreases with phosphor coating weight. A similar but much less pronounced behavior is observed for the 80 kVp curve, reaching maximum at 100 mg/cm^2 ; 80 kVp X-rays are more penetrating reaching saturation at higher coating weights.

Figure 4 shows the $\text{DQE}(\omega)$ variation with spatial frequency for all $\text{YVO}_4:\text{Eu}$ screens measured at 80 kVp. At medium and high frequencies DQE decreases with coating weight due to the pronounced light spread within the phosphor material, which causes a reduction in MTF and consequently in DQE [see relation (3)]. However, at low frequen-

cies, where the MTF values of all screens converge (see Fig. 1), η_ϕ and η_Q play a predominant role in the DQE value. This explains the low DQE of the 30 mg/cm^2 screen in the low frequency range. However, as frequency increases the DQE of the 30 mg/cm^2 screen decreases slower than the other screens, due to its significantly higher MTF (see Fig. 1). A similar behavior is observed for the 60 mg/cm^2 screen in the low frequency range close to zero.

Figure 5 compares the DQEs of the 30 mg/cm^2 $\text{YVO}_4:\text{Eu}$ screen measured at 30 kVp with that of the 80 mg/cm^2 screen at 80 kVp. As it is shown the 30 mg/cm^2 -30 kVp DQE is considerably higher in the whole frequency range, thus demonstrating the satisfactory imaging performance of $\text{YVO}_4:\text{Eu}$ at mammographic conditions. Additionally, the 30 mg/cm^2 -30 kVp curve is clearly higher than the DQE curves shown in Fig. 4 corresponding to 80 kVp. The superiority of this DQE is due to the combined effects of (1) the high X-ray absorption caused by the proximity of yttrium's K -edge to the beam's mean energy and (2) the low light attenuation and light spread in thin screens.

Acknowledgements—This study is dedicated to the memory of Professor G. E. Giakoumakis, leading member of our team, whose work on phosphor material has inspired us to continue.

REFERENCES

- Arnold, B. A. (1979) Physical characteristics of screen-film combinations. In *The Physics of Medical Imaging: Recording System, Measurements and Techniques*, ed.

- A. G. Haus, pp. 30–71. American Association of Physicists in Medicine, New York.
- Barnes, G. T. (1979) The use of bar pattern test objects in assessing the resolution of film/screen systems. In *The Physics of Medical Imaging Recording System Measurements and Techniques*, ed. A. G. Haus, pp. 138–151. American Association of Physicists in Medicine, New York.
- Beutel, J., Mickewich, D. J., Issler, S. L. and Shaw, R. (1993) The image quality characteristics of a novel ultra-high-resolution film/screen system. *Phys. Med. Biol.* **38**, 1195–1206.
- Bunch, P. C., Huff, K. E. and Van Metter, R. (1987) Analysis of detective quantum efficiency of a radiographic film-screen combination. *J. Opt. Soc. Am.* **A4**, 902–909.
- Cavouras, D., Kandarakis, I., Panayiotakis, G., Evangelou, E. K. and Nomicos, C. D. (1996) An evaluation of the $\text{Y}_2\text{O}_3:\text{Eu}^{3+}$ scintillator for application in medical x-ray detectors and image receptors. *Med. Phys.* **23**, 1965–1975.
- Giakoumakis, G. E. (1991) Matching factors for various light-source-photodetector combinations. *Appl. Phys.* **A52**, 7–9.
- Gurwich, A. M. (1995) Luminescent screens for mammography. *Radiat. Meas.* **24**, 325–330.
- Hendee, W. R. (1970) *Medical Radiation Physics*, pp. 145–148. Year Book Medical Publishers, Chicago.
- Kandarakis, I., Cavouras, D., Panayiotakis, G., Agelis, T., Nomicos, C. and Giakoumakis, G. (1996) X-ray induced luminescence and spatial resolution of $\text{La}_2\text{O}_2\text{S}:\text{Tb}$ phosphor screens. *Phys. Med. Biol.* **41**, 297–307.
- Kandarakis, I., Cavouras, D., Panayiotakis, G. S. and Nomicos, C. (1997a) Evaluating X-ray detectors for radiographic applications: a comparison of $\text{ZnScdS}:\text{Ag}$ with $\text{Gd}_2\text{O}_2\text{S}:\text{Tb}$ and $\text{Y}_2\text{O}_2\text{S}:\text{Tb}$ screens. *Phys. Med. Biol.* **42**, 1351–1373.
- Kandarakis, I., Cavouras, D., Panayiotakis, G. S., Triantis, D. and Nomicos, C. D. (1997b) An experimental method for the determination of spatial frequency dependent detective quantum efficiency (DQE) of scintillators used in x-ray imaging detectors. *Nucl. Instr. and Meth. Phys. Res.* **A399**, 345–342.
- Ludwig, G. W. (1971) X-ray efficiency of powder phosphors. *J. Electrochem. Soc.* **118**, 1152–1159.
- Motz, J. W. and Danos, M. (1978) Image information content and patient exposure. *Med. Phys.* **5**, 8–22.
- Panayiotakis, G., Cavouras, D., Kandarakis, I. and Nomicos, C. (1996) A study of X-ray luminescence and spectral compatibility of europium-activated yttrium-vanadate ($\text{YVO}_4:\text{Eu}$) screens for medical imaging applications. *Appl. Phys.* **62**, 483–486.
- Storm, E. and Israel, H. (1967) *Photo cross-sections from 0.001 to 100 MeV for elements 1 through 100 Report LA-3753*. Los Alamos Scientific Laboratory, University of California.
- Shaw, R. (1963) The equivalent quantum efficiency of the photographic process. *J. Photogr. Sci.* **11**, 199–204.
- Shaw, R. and Van Metter, R. (1984) An analysis of the fundamental limitations of screen-film systems for X-ray detection. *Proc. SPIE* **454**, 128–132.
- Tucker, D. M., Barnes, G. T. and Wu, X. (1991a) Molybdenum target X-ray spectra: A Semiempirical model. *Med. Phys.* **18**, 402–407.
- Tucker, D. M., Barnes, G. T. and Chakraborty, D. B. (1991b) Semi-empirical model for generating tungsten target X-ray spectra. *Med. Phys.* **18**, 211–218.
- Yaffe, M. J. and Rowlands, J. A. (1997) X-ray detectors for digital radiography. *Phys. Med. Biol.* **42**, 1–39.
- Zweig, G. and Zweig, D. A. (1983) Radioluminescent imaging: factors affecting total light output. *Proc. SPIE* **419**, 297–304.

APPENDIX

The mean number of light photons \bar{m}_0 produced within the phosphor material per X-ray quantum absorbed is given by:

$$\bar{m}_0 = \eta_C \left[\frac{\bar{E}}{E_i} \right] \quad (\text{A1})$$

where η_C is the intrinsic X-ray to light conversion efficiency giving the fraction of X-ray energy flux that is converted into light energy flux within the phosphor material. \bar{E} , E_i are the corresponding mean energies of the incident X-ray photons and emitted light photons.

The mean number N_L of light photons emitted by a phosphor screen excited by N_X X-rays incident per unit of area and time is given by the following relation (Shaw and Van Metter, 1984; Bunch *et al.*, 1987):

$$N_L = N_X \eta_Q \bar{m}_0 G \quad (\text{A2})$$

where η_Q is the X-ray quantum detection efficiency of the phosphor. G is the fraction of produced light photons that are transmitted through the material and are emitted from the surface of the phosphor.

The X-ray luminescence efficiency of a phosphor (η_ϕ) is defined (Ludwig, 1971) as the ratio of the light energy flux Ψ_L emitted over the incident X-ray energy flux Ψ_X :

$$\eta_\phi = \Psi_L / \Psi_X \quad (\text{A3})$$

where

$$\Psi_L = N_L E_i \quad \text{and} \quad \Psi_X = N_X \bar{E}. \quad (\text{A4})$$

From relations (A1)–(A3) it is obtained that

$$N_L = N_X \eta_Q \eta_C [\bar{E}/\bar{E}_i] G = N_X \eta_\phi [\bar{E}/\bar{E}_i] \quad (\text{A5})$$

which is obtained using relation $\eta_\phi = \eta_Q \eta_C G$ (Ludwig, 1971).

The spatial frequency dependent DQE of a phosphor has been described (Shaw, 1963; Shaw and Van Metter, 1984) in terms of the modulation transfer function MTF and the noise power spectrum NPS as follows:

$$\text{DQE}(\omega) = N_X [dN_L/dN_X]^2 \frac{\text{MTF}^2(\omega)}{\text{NPS}(\omega)}. \quad (\text{A6})$$

NPS may be expressed (Shaw and Van Metter, 1984) as:

$$\text{NPS}(\omega) = N_X \eta_Q [\bar{m}_0 G]^2 \text{MTF}^2(\omega) + N_L. \quad (\text{A7})$$

From (A1)–(A7) it is obtained that

$$\text{DQE}(\omega) = \frac{\eta_Q \eta_\phi [\bar{E}/E_i] [\text{MTF}]^2}{\eta_Q + \eta_\phi [\bar{E}/E_i] [\text{MTF}]^2}. \quad (\text{A8})$$